Current Biology, Vol. 12, 329–334, February 19, 2002, ©2002 Elsevier Science Ltd. All rights reserved. PII S0960-9822(02)00654-1

Cell Polarity Signaling in *Arabidopsis* Involves a BFA-Sensitive Auxin Influx Pathway

Markus Grebe,[1] Jiří Friml,[3,7] Ranjan Swarup,[4] Karin Ljung,[5] Göran Sandberg,[5] Maarten Terlou,[2] Klaus Palme,[3] Malcolm J. Bennett,[4] and Ben Scheres[1,6]

[1] Department of Molecular Cell Biology and
[2] Department of Image Processing and Design
Utrecht University
Padualaan 8
3584 CH Utrecht
The Netherlands
[3] Max-Delbrück-Laboratorium in der
Max-Planck-Gesellschaft
Carl-von-Linne-Weg 10
D-50829 Köln
Germany
[4] School of Biological Sciences
University Park
University of Nottingham
NG7 2RD Nottingham
United Kingdom
[5] Umeå Plant Science Center
Department of Forest Genetics and
Plant Physiology
The Swedish University of Agricultural Sciences
S-901083 Umeå
Sweden

Summary

Coordination of cell and tissue polarity commonly involves directional signaling [1]. In the *Arabidopsis* root epidermis, cell polarity is revealed by basal, root tip-oriented, hair outgrowth from hair-forming cells (trichoblasts) [2]. The plant hormone auxin displays polar movements [1, 3] and accumulates at maximum concentration in the root tip [4, 5]. The application of polar auxin transport inhibitors [3] evokes changes in trichoblast polarity only at high concentrations and after long-term application [2, 4]. Thus, it remains open whether components of the auxin transport machinery mediate establishment of trichoblast polarity. Here we report that the presumptive auxin influx carrier AUX1 [6, 7] contributes to apical-basal hair cell polarity. *AUX1* function is required for polarity changes induced by exogenous application of the auxin 2,4-D, a preferential influx carrier substrate. Similar to *aux1* mutants, the vesicle trafficking inhibitor brefeldin A (BFA) interferes with polar hair initiation, and *AUX1* function is required for BFA-mediated polarity changes. Consistently, BFA inhibits membrane trafficking of AUX1, trichoblast hyperpolarization induced by 2,4-D, and alters the distal auxin maximum. Our results identify AUX1 as one component of a novel BFA-sensitive auxin transport pathway polarizing cells toward a hormone maximum.

[6] Correspondence: b.scheres@bio.uu.nl
[7] Present address: Entwicklungsgenetik, Zentrum für Molekularbiologie der Pflanzen, Universität Tübingen, Auf der Morgenstelle 3, D-72076 Tübingen, Germany.

Results and Discussion

Polar auxin transport has been implicated in the coordination of plant cell and organ polarity [1] and is thought to be mediated by auxin efflux carriers [3, 8]. The *Arabidopsis* PIN1 and PIN2 (also called EIR1/AGR1) proteins represent two presumptive efflux carriers [9–13]. Consistent with this proposed function, *pin1* and *pin2* mutants show defects attributed to disturbed polar auxin transport, such as disturbances in vascular strand formation or root gravitropism [9–13]. Moreover, the asymmetric plasma membrane distribution of both proteins correlates with proposed routes of polar auxin transport [8–10]. A second carrier system facilitates auxin influx into plant cells [14] and *Arabidopsis* AUX1 represents a presumptive influx carrier [5, 6]. Recently, polar and axial localization of AUX1 has been reported for root vascular and epidermis cells [15]. These observations raise the question whether, contrary to present views, the influx carrier system contributes to the regulation of cell polarity.

To causally assess an involvement of auxin transporters in establishment of apical-basal trichoblast polarity, we analyzed *Arabidopsis eir1* and *aux1* mutants for defects in this process. We applied two criteria for changes in trichoblast polarity: apical-basal shifting of hair initiation and formation of double hairs from trichoblasts. Both markers are invariable in wild-type and can be reliably quantified [2]. Three *aux1* mutant alleles analyzed displayed apical shifting of hair initiation (Figures 1B, 1F, 1G, and 1L) and a low frequency of double hair formation that, nonetheless, was ~30 times higher than in the wild-type (Figures 1C and 1D, Table 1). By contrast, *eir1* mutants defective in epidermally expressed PIN2 protein [10, 11] did not reveal changes in apical-basal trichoblast polarity (Figures 2E and 2I; Table 1). Loss of *AUX1* function caused the observed phenotypes, since the defects were rescued in *aux1* seedlings transformed with the wild-type genomic *AUX1* sequence carrying an insertion for an HA-epitope tag (Figures 1H and 1I; Table 1). These results provide the first link between a molecular component of the auxin transport machinery and establishment of apical-basal epidermal polarity in *Arabidopsis*.

We further examined the contributions of different auxin transport systems by external application of auxin analogs, which are differentially transported by influx and efflux carriers [14]. The synthetic auxin 2,4-dichlorophenoxyacetic acid (2,4-D) constitutes a preferential substrate for the auxin influx system, while 1-naphthalene acetic acid (1-NAA) enters cells by diffusion and is efficiently exported by the efflux system [14]. Seedlings grown on 20 nM 2,4-D initiated root hairs from a more basal position than untreated controls (Figures 1E and

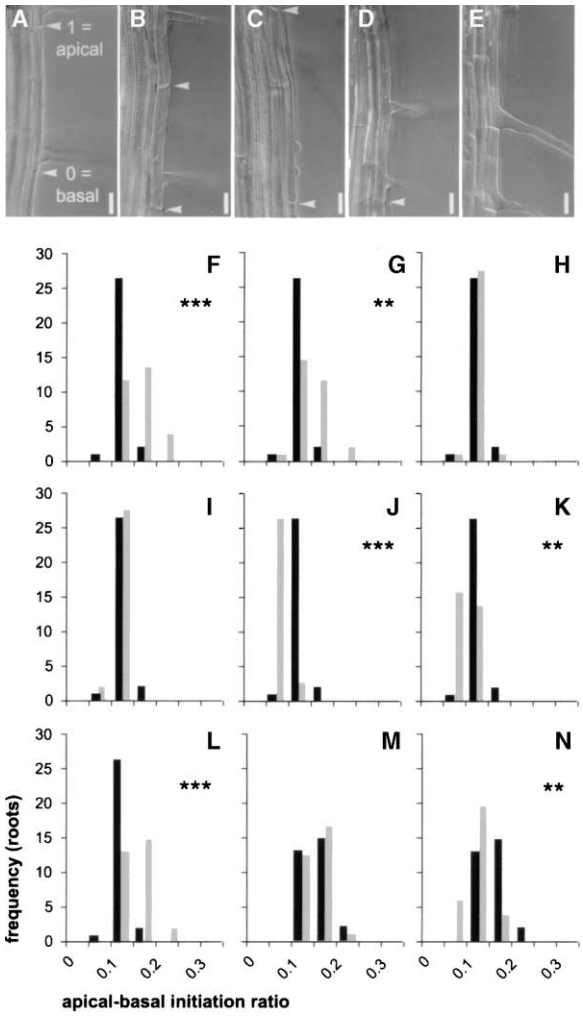

Figure 1. *aux1* Mutations and Exogenous Auxin Application Affect Trichoblast Polarity

(A) *Arabidopsis* trichoblasts wild-type Columbia (Col). (A–D) White arrowheads, cell walls. Scale bars, 20 μm. (B and C) *aux1-7*. (D) *aux1-21*. (E) Col 20 nM 2,4-D. (F–N) Frequency distributions of average hair initiation per root (30 roots, 150 trichoblasts each). Apical-basal initiation ratios indicate relative positions of hair initiation. 0 = basal, 1 = apical, compare to (A). (F–L) Col wild-type control (black). (F) *aux1-21* (gray). (G) *aux1-22* (gray). (L) *aux1-7* (gray). (I) *aux1-7AUX1* (gray). (H) *aux1-22HA-AUX1* (gray). (J) Col 20nM 2,4-D (gray). (K) Col 100 nM 1-NAA (gray). (M–N) *aux1-7* control (black). (M) *aux1-7* 20 nM 2,4-D (gray). (N) *aux1-7* 100 nM 1-NAA (gray). Significance level for independence of distributions is $p < 0.05$. p values are indicated as highly significant: $^{**}p \leq 0.001$ and $^{***}p \leq 0.0001$.

1J). We refer to basal shifting of hair initiation as trichoblast "hyperpolarization." The influx carrier substrate 2,4-D exerted hyperpolarizing activity in a concentration range similar to the naturally occurring auxin indole-3-acetic acid (IAA) [2]. In contrast, higher 1-NAA concentrations (100 nM 1-NAA) were required to induce trichoblast hyperpolarization (Figure 1K; Table 1). The uptake of 2,4-D and IAA into *Arabidopsis* root tips required *AUX1* function [7, 16]. Therefore, we reasoned that 2,4-D action on apical-basal trichoblast polarity might also involve *AUX1* activity. Consistent with this assumption, *aux1* seedlings were resistant to 2,4-D-promoted trichoblast hyperpolarization and maintained double hair formation (Figure 1M; Table 1). By contrast, 1-NAA rescued the *aux1* double hair phenotype and conferred partial basal hair shifting (Figure 1N; Table 1). The 1-NAA-mediated rescue of the *aux1* phenotype suggests that polar hair initiation either involves additional, as yet unidentified, efflux components or that increasing the intracellular auxin concentration in the trichoblast is sufficient to correct the *aux1* polarity defects. Nevertheless, trichoblast hyperpolarization induced by 2,4-D required *AUX1* activity which identifies AUX1 as an influx carrier component mediating apical-basal polarity.

Polar auxin transport inhibitors strongly interfered with trichoblast polarity only after long-term application at high concentrations [2, 4]. To uncover more specific modulators, we examined effects of different auxin transport and membrane trafficking inhibitors [17–19]. The vesicle trafficking inhibitor brefeldin A (BFA) [20] most strongly and specifically affected apical-basal trichoblast polarity in a concentration-dependent manner. BFA (1 μM) induced subtle but clear apical shifting of hair initiation (Figures 2B and 2E), while 2.5 μM BFA caused strong apical shifting in extreme cases resulting in hair formation from apical trichoblast ends (Figures 2C and 2F). Additionally, this concentration induced double hair formation at low frequency (Figure 2D; Table 1). Thus, a BFA-sensitive pathway is required for establishment of apical-basal polarity in the *Arabidopsis* root epidermis.

Hitherto, BFA was believed to interfere with the auxin efflux but not the influx carrier machinery, as concluded from auxin transport experiments on plant cell cultures and tissue segments [18, 19, 21]. Consistent with action on efflux carriers, BFA abolishes polar membrane localization and cycling of *Arabidopsis* PIN1 [22, 23]. In light of the similar phenotypes induced by BFA application and *aux1* mutation, we addressed whether BFA might interact with *AUX1* during establishment of trichoblast polarity. In *aux1* mutants, apical shifting could not be enhanced by 1 μM BFA (Figure 2G), and *aux1* conferred partial resistance to the effect of 2.5 μM BFA (Figure 2H) when compared to wild-type (Figures 2E and 2F) and *eir1* mutants (Figures 2I and 2J) (see also Table 1). Thus, *AUX1* function is required for BFA action on trichoblast polarity suggesting AUX1 as one component of a BFA-sensitive pathway.

We further examined whether BFA affects 2,4-D action on trichoblast polarity. Concomitant application of 20 nM 2,4-D and 1 μM BFA completely inhibited the hyperpolarizing activity of 2,4-D (Figure 2K; Table 1). By contrast, 100 nM 1-NAA induced basal shifting when applied together with BFA (Figure 2L; Table 1). BFA inhibition of 2,4-D action further supported that auxin influx components act in a BFA-sensitive pathway.

We reasoned that AUX1 membrane trafficking might be a target for BFA interference and immunolocalized the functional HA-AUX1 fusion protein (Figure 1H) [15] after incubation of seedlings with BFA. As reported previously, in control roots, AUX1 localized to apical ends of protophloem cells (Figures 3A and 3B) as well as apical and basal ends of epidermal cells (Figures 3C and 3D) [15]. BFA treatment resulted in disruption of

Table 1. Quantitative Effects of Mutations in Auxin Transporters, Auxin, and BFA Treatments on Apical-Basal Cell Polarity

	Cell Length (μm)	Initiation Length (μm)	Apical-Basal Initiation Ratio	Double Hairs (%)
Col	156 ± 14	18 ± 1	0.12 ± 0.005	0.1 (n = 3000)
eir1-1	186 ± 12	21 ± 2	0.12 ± 0.01	0.2 (n = 3000)
aux1-7	168 ± 4	26 ± 2	0.16 ± 0.02	2.9 (n = 2000)
aux1-21	170 ± 17	29 ± 2	0.17 ± 0.01	2.9 (n = 3000)
aux1-22	185 ± 6	28 ± 2	0.15 ± 0.01	3.1 (n = 3000)
aux1-22 HA-AUX1	145 ± 11	18 ± 3	0.12 ± 0.01	0.1 (n = 3000)
aux1-7 AUX1	174 ± 9	20 ± 1	0.12 ± 0.01	ND
Col 10 nM 2,4-D	154 ± 6	15 ± 1	0.10 ± 0.003	0 (n = 3000)
Col 20 nM 2,4-D	114 ± 10	10 ± 1	0.09 ± 0.002	0 (n = 3000)
aux1-7 20 nM 2,4-D	177 ± 6	27 ± 1	0.155 ± 0.005	3.0 (n = 2700)
aux1-7 100 nM 1-NAA	149 ± 8	18 ± 1	0.12 ± 0.01	0.1 (n = 3000)
Col 100 nM 1-NAA	128 ± 13	12 ± 1	0.095 ± 0.003	0 (n = 3000)
Col 1 μM BFA	160 ± 8	27 ± 3	0.17 ± 0.01	0.5 (n = 3000)
Col 2.5 μM BFA	138 ± 9	46 ± 5	0.34 ± 0.04	1.3 (n = 2000)
aux1-7 1 μM BFA	179 ± 10	25 ± 2	0.14 ± 0.01	2.6 (n = 2500)
aux1-7 2.5 μM BFA	161 ± 9	44 ± 4	0.28 ± 0.03	3.4 (n = 2200)
aux1-22 1 μM BFA	186 ± 3	26 ± 2	0.14 ± 0.01	ND
aux1-22 2.5 μM BFA	170 ± 3	45 ± 4	0.27 ± 0.03	ND
eir1-1 1 μM BFA	170 ± 2	28 ± 3	0.17 ± 0.01	ND
eir1-1 2.5 μM BFA	195 ± 7	70 ± 11	0.36 ± 0.05	1.2 (n = 3000)
Col 20 nM 2,4-D 1 μM BFA	141 ± 6	24 ± 3	0.17 ± 0.01	0.4 (n = 3000)
Col 100 nM 1-NAA 1 μM BFA	126 ± 6	17 ± 2	0.13 ± 0.01	0 (n = 3000)

Data are means derived from three independent experiments including 50 cells from 10 roots each. Standard deviations are indicated. For double hair analyses, n = total numbers of cells analyzed are indicated. ND, not determined.

AUX1 plasma membrane localization (Figures 3E–3H). In protophloem cells, AUX1-positive material coalesced into intracellular patches (Figures 3E and 3F) similar to previously described "BFA compartments" [22–24]. In BFA-treated epidermal cells, AUX1 label displayed a more uniform cytoplasmic distribution (Figures 3G and 3H). Additionally, BFA affected AUX1 staining in columella cells and AUX1 membrane localization in lateral root cap cells (data not shown). We conclude that membrane trafficking of AUX1 is sensitive to BFA interference and suggest that BFA may act on AUX1 localization during establishment of trichoblast polarity.

We finally addressed whether BFA affects the endogenous auxin distribution in the root tip. We employed transgenic plants harboring auxin-responsive promoters fused to the *GUS* reporter gene [4, 15, 25] to estimate local changes in auxin responses. Additionally, we determined free auxin levels in the root tip by high-resolution gas chromatography-selected reaction monitoring-mass spectrometry (GC-SRM-MS) [26]. Expression of the auxin-responsive *DR5::GUS* reporter (Figure 3I) was enhanced in upper columella cells in seedlings grown on 2.5 μM BFA (Figure 3J). Similarly, GC-SRM-MS measurements demonstrated an increase of free IAA in the distal millimeter of the root at this BFA concentration (Figure 3K). The *IAA2::GUS* reporter gene (Figure 3L) revealed a weak but consistent increase of expression in the quiescent center and upper columella cells under BFA treatment (Figure 3M). Together, these results suggest BFA action on auxin redistribution from the distal auxin maximum.

Our observations indicate that at least one molecular component of the auxin transport machinery, AUX1, constitutes part of a system polarizing epidermal cells toward a hormone maximum. Three independent lines of evidence presented suggest that, contrary to current views, the influx carrier system is subject to BFA interference. It remains open which part of the AUX1 expression domain mediates establishment of trichoblast polarity and BFA-induced polarity changes. We are currently constructing clonal analysis systems to clarify this point. Our observations are consistent with two models. First, changes in trichoblast polarity may result from a disturbed relay of auxin transport from protophloem, columella, or lateral root cap cells toward the polarizing trichoblast. Thus, they may involve disturbance of non-cell-autonomous *AUX1* function. Alternatively, our results can be explained by defects in cell-autonomous *AUX1* function and BFA interference with AUX1 in the polarizing trichoblast. The finding that AUX1 mediates acropetal and basipetal auxin transport would be consistent with both hypotheses [15]. Based on the epidermal polarity defects in *aux1*, AUX1 localization in epidermal cells, and the requirement of *AUX1* function for BFA action on this cell layer, we favor the following model. The distal auxin maximum provides an organizing cue for polarization of epidermal cells, and AUX1 relays this information in the polarizing trichoblast by establishing an inter- or intracellular concentration difference.

The subtle phenotype and the partial resistance of *aux1* mutants to higher BFA concentrations suggest that such a signal relay involves additional components. Accordingly, changes in the distal auxin maximum occurred at BFA concentrations to which *aux1* conferred only partial resistance. Therefore, it remains open which other BFA-sensitive factors are involved in establishment of epidermal polarity and whether changes in the auxin maximum account for the observed polarity phenotypes. Additional, as yet to be identified, BFA-sensitive components may cooperate to transport and sense a directional auxin cue from the distal maximum and include factors mediating overt features of cell polarity in the polarizing trichoblast. Consistent with the latter view, polar localization of Rop-type GTPases to the in-

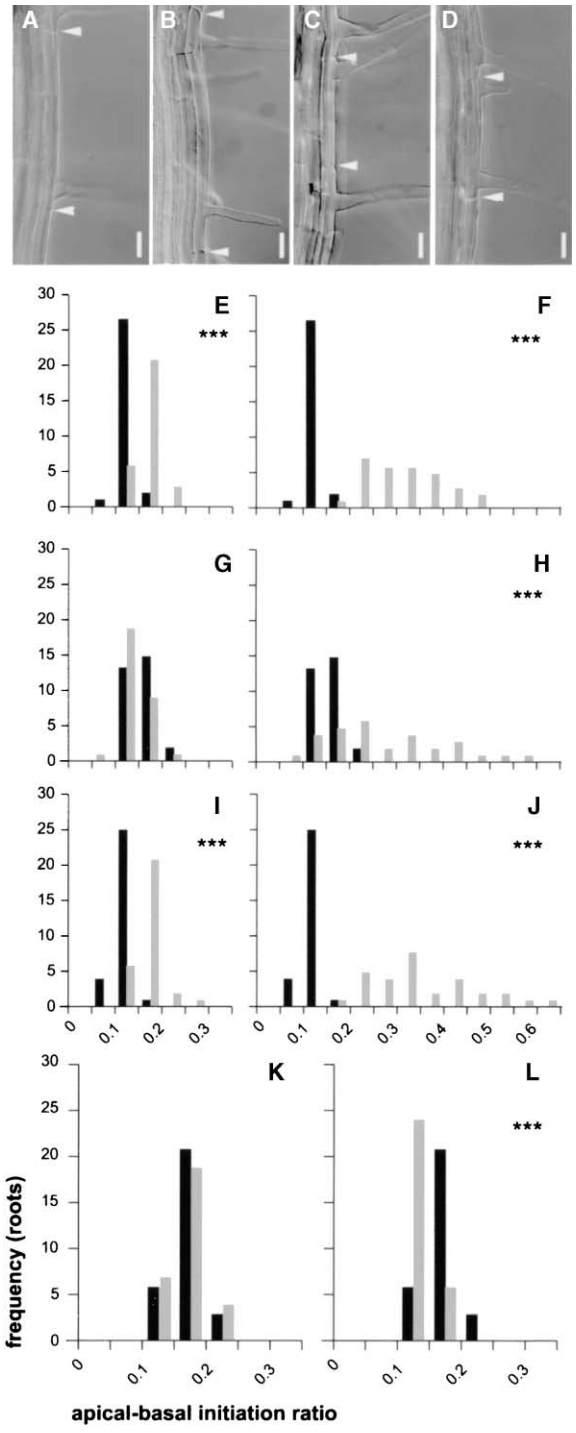

Figure 2. BFA Changes Trichoblast Polarity and Acts on Auxin Influx Components

(A–D) *Arabidopsis* seedlings grown on BFA or auxins as indicated. (A) Col trichoblasts as of Figure 1A. (A–D) White arrowheads, cell walls. Scale bars, 20 μm. (B) Col 1 μM BFA. (C and D) Col 2.5 μM BFA. (E–L) Frequency distributions of apical-basal hair initiation per root (compare Figure 1). (E and F) Col (black). (E) Col 1 μM BFA (gray). (F) Col 2.5 μM BFA (gray). (G and H) *aux1-7* control (black). (G) *aux1-7* 1 μM BFA (gray). (H) *aux1-7* 2.5 μM BFA (gray). Note that (H) *aux1-7* 2.5 μM BFA (gray) is different from (F) Col 2.5 μM BFA (gray) ($p \leq 0.01$). (I and J) *eir1-1* (black). (I) *eir1-1* 1 μM BFA (gray). (J) *eir1-1* 2.5 μM BFA (gray). Note that (I) *eir1-1* (black) is similar to (E) Col (black) ($p = 0.71$). (K) Col 1 μM BFA (black) Col 20 nM 2,4-D 1 μM BFA (gray). (L) Col 1 μM BFA (black); Col 100 nM 1-NAA 1 μM BFA (gray).

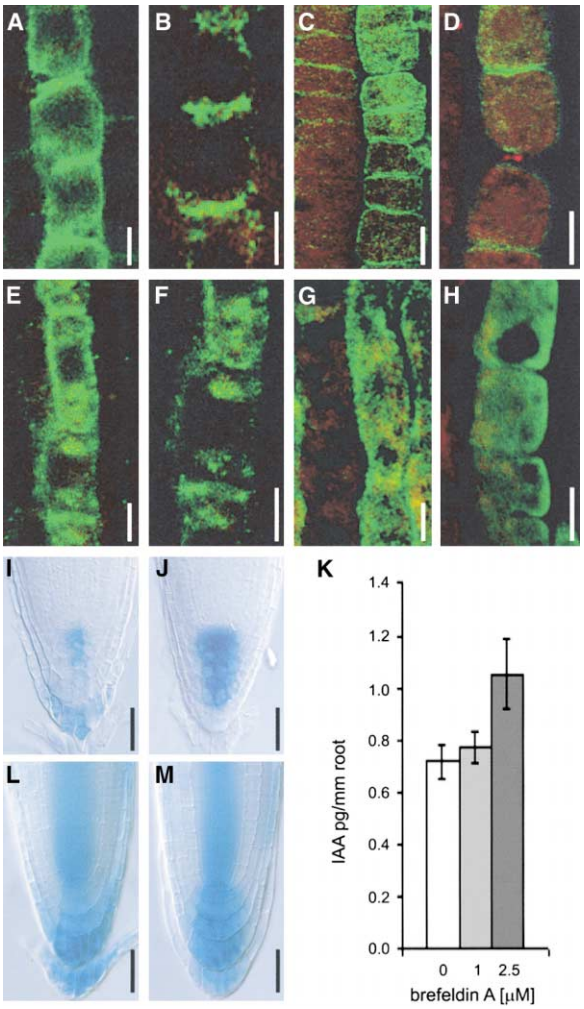

Figure 3. BFA Interferes with AUX1 Localization and Auxin Distribution

(A–H) Localization of HA-tagged AUX1 (HA-AUX1) in *aux1-22* mutant background. (A–D) DMSO controls. (A and B) Protophloem cells. (C and D) Epidermis cells. (E–H) Treatment with 100 μM BFA for 3 hr. (E and F) Protophloem cells. (G and H) Epidermal cells. (A–H) Scale bars, 10 μm. (I and J) Root tip-localized *DR5::GUS* expression in 5-day-old seedlings. (I) DMSO control. (J) 2.5 μM BFA. (K) GC-SRM-MS analysis of IAA accumulation in the first 1 mm of the root in day 5 seedlings. (L and M) Root tip-localized *IAA2::GUS* expression in day 5 seedlings. (L) DMSO control. (M) Seedlings grown on 2.5 μM BFA.

cipient site of hair initiation has recently been shown to provide an additional target for BFA interference [27].

Experimental Procedures

Plant Material and Growth Conditions

aux1 and *eir1* mutant alleles, *HA*-tagged, and non-tagged *AUX1* genomic rescue constructs have been described previously [6, 11, 15, 28, 29]. Seeds were sterilized and imbibed, then germinated on

vertically oriented plates containing 1/2 MS agar, 1% sucrose (pH 5.8) under conditions described previously [30]. Trichoblast phenotypes, reporter gene expression, and immunolocalization studies were carried out on 5-day-old seedlings.

Hormone and Inhibitor Treatments

Inhibitors or auxins were added to agar at 60°C after autoclaving: 0.1–10 μM BFA (Sigma) from a 50 mM stock in dimethylsulfoxide (DMSO), 10–300 nM 1-NAA (Sigma) from a 100 mM stock in 1 N NaOH, 10–200 nM 2,4-D from a 10 mM stock in 70% EtOH (Sigma). Screening for polarity phenotypes was at 50× magnification using a Zeiss stereomicroscope (Stemi SV6). Mutants displaying and conditions inducing specific polarity changes were selected for quantitative microscopic analysis.

Quantitative Microscopic, Image, and Statistical Analysis

Seedlings mounted in chloral hydrate [30] were analyzed for double hair formation by Nomarski optics using a Zeiss Axioskop. Per mutant or treatment, a total of 2000 to 3000 trichoblasts were analyzed quantitatively in at least three independent experiments and qualitatively observed for their cell and initiation lengths (distance from the center of root hair outgrowth to the basal cell wall). Quantification of apical-basal shift phenotypes was performed for 150 differentiated trichoblasts derived from three experiments, each involving 50 cells from 10 roots. Specimens were viewed under a Zeiss Mikroskop II, scanned with a CCD camera (Panasonic WC-CD50), and analyzed with an image analysis system (IBAS, Carl Zeiss Vision, München, Germany) employing software available on request from M.T. Statistical analysis is presented on a per root basis, since polar hair initiation in *Arabidopsis* is a coordinated event [2]. Analysis on a per cell basis revealed similar results. Relative positions of hair initiation were determined as apical-basal initiation ratio = initiation length (μm)/cell length (μm). The average initiation ratio per root was determined from ratios of five cells. Class distributions were analyzed for 30 roots. Statistical analysis for independence of distributions were based on Fisher's exact test applying the "Fisher 2 by 5" program (http://home.clara.net/sisa/).

Whole-Mount Immunofluorescence Analysis on Root Tips

Seedlings were incubated in BFA-containing medium [22] or with appropriate volumes of DMSO for 1–3 hr and fixed for 30 min. AUX1 immunolocalization and visualization was performed as described [15, 22]. Antibody concentrations were 1:200 for anti-HA antibody (BAbCO) and 1:200 for anti-mouse FITC-coupled secondary antibody (Sigma).

Histochemical Analysis of β-Glucuronidase Activity

β-glucuronidase (GUS) activity was visualized by staining for 25 min for *DR5::GUS* or 60 min for *IAA2::GUS* at 37°C as described [30], in three to seven independent experiments each employing at least ten roots.

Detection of Free IAA in Root Tips by GC-SRM-MS

Free IAA concentrations in the most distal 1 mm section of root tips were analyzed by GC-SRM-MS as described [26], including slight modifications [15].

Acknowledgments

We thank J.R. Ecker and the *Arabidopsis* Stock Center for providing *eir1* and *aux1* mutant alleles; and F. Frugier, M. Proveniers, W.-A. Rensink, and D. Welch for critical reading of the manuscript. This work was supported by a PIONIER award of the Dutch Organization for Sciences (NWO) to B.S. and by a Marie Curie postdoctoral fellowship (HPMF-CT-2000-00969) of the European Community Framework Programme V to M.G.

Received: October 20, 2001
Revised: December 19, 2001
Accepted: December 19, 2001
Published: February 19, 2002

References

1. Sachs, T. (1991). Cell polarity and tissue patterning in plants. Development Suppl. *1*, 83–93.
2. Masucci, J.D., and Schiefelbein, J.W. (1994). The *rhd6* mutation of *Arabidopsis thaliana* alters root hair initiation through an auxin- and ethylene-associated process. Plant Physiol. *106*, 1335–1346.
3. Lomax, T.L., Muday, G.K., and Rubery, P.H. (1995). Auxin transport. In Plant Hormones: Physiology, Biochemistry and Molecular Biology, P.J. Davies, ed. (Dordrecht: Kluwer Academic Publishers), pp. 509–530.
4. Sabatini, S., Beis, D., Wolkenfelt, H., Murfett, J., Guilfoyle, T., Malamy, J., Benfey, P., Leyser, O., Bechtold, N., Weisbeek, P., et al. (1999). An auxin-dependent distal organiser of pattern and polarity in the *Arabidopsis* root. Cell *99*, 463–472.
5. Casimiro, I., Marchant, A., Bhalerao, R.P., Beeckman, T., Dhooge, S., Swarup, R., Graham, N., Inze, D., Sandberg, G., Casero, P.J., et al. (2001). Auxin transport promotes *Arabidopsis* lateral root initiation. Plant Cell *13*, 843–852.
6. Bennett, M.J., Marchant, A., Green, H.G., May, S.T., Ward, S.P., Millner, P.A., Walker, A.R., Schulz, B., and Feldmann, K.A. (1996). *Arabidopsis AUX1* gene: A permease-like regulator of root gravitropism. Science *27*, 948–950.
7. Marchant, A., Kargul, J., May, S.T., Muller, P., Delbarre, A., Perrot-Rechenmann, C., and Bennett, M.J. (1999). *AUX1* regulates root gravitropism in *Arabidopsis* by facilitating auxin uptake within root apical tissues. EMBO J. *18*, 2066–2073.
8. Leyser, O. (1999). Plant hormones: ins and outs of auxin transport. Curr. Biol. *9*, R8–R10.
9. Gälweiler, L., Guan, C., Müller, A., Wisman, E., Mendgen, K., Yephremov, A., and Palme, K. (1998). Regulation of polar auxin transport by AtPIN1 in *Arabidopsis* vascular tissue. Science *282*, 2226–2230.
10. Muller, A., Guan, C., Galweiler, L., Tanzler, P., Huijser, P., Marchant, A., Parry, G., Bennett, M., Wisman, E., and Palme, K. (1998). *AtPIN2* defines a locus of *Arabidopsis* for root gravitropism control. EMBO J. *17*, 6903–6911.
11. Luschnig, C., Gaxiola, R.A., Grisafi, P., and Fink, G.R. (1998). *EIR1*, a root specific protein involved in auxin transport, is required for gravitropism in *Arabidopsis thaliana*. Genes Dev. *12*, 2175–2187.
12. Chen, R.J., Hilson, P., Sedbrook, J., Rosen, E., Caspar, T., and Masson, P.H. (1998). The *Arabidopsis thaliana AGRAVITROPIC* 1 gene encodes a component of the polar-auxin-transport efflux carrier. Proc. Natl. Acad. Sci. USA *95*, 15112–15117.
13. Utsuno, K., Shikanai, T., Yamada, Y., and Hashimoto, T. (1998). *AGR*, an agravitropic locus of *Arabidopsis thaliana*, encodes a novel membrane-protein family member. Plant Cell Physiol. *39*, 1111–1118.
14. Delbarre, A., Muller, P., Imhoff, V., and Guern, J. (1996). Comparison of mechanisms controlling uptake and accumulation of 2,4-dichlorophenoxy acetic acid, naphthalene-1-acetic acid, and indole-3-acetic acid in suspension-cultured tobacco cells. Planta *198*, 532–541.
15. Swarup, R., Friml, J., Marchant, A., Ljung, K., Sandberg, G., Palme, K., and Bennett, M. (2001). Localization of the auxin permease AUX1 suggests two functionally distinct hormone transport pathways operate in the *Arabidopsis* root apex. Genes Dev. *15*, 2648–2653.
16. Rahman, A., Ahamed, A., Amakawa, T., Goto, N., and Tsurumi, S. (2001). Chromosaponin I specifically interacts with AUX1 protein in regulating the gravitropic response of *Arabidopsis* roots. Plant Physiol. *125*, 990–1000.
17. Imhoff, V., Muller, P., Guern, J., and Delbarre, A. (2000). Inhibitors of the carrier-mediated influx of auxin in suspension-cultured tobacco cells. Planta *210*, 580–588.
18. Delbarre, A., Muller, P., and Guern, J. (1998). Short-lived and phosphorylated proteins contribute to carrier-mediated efflux, but not to influx, of auxin in suspension-cultured tobacco cells. Plant Physiol. *116*, 833–844.
19. Morris, D.A., and Robinson, J.S. (1998). Targeting of auxin carriers to the plasma membrane: differential effects of brefeldin A on the traffic of auxin uptake and efflux carriers. Planta *205*, 606–612.

20. Satiat-Jeunemaitre, B., Cole, L., Bourett, T., Howard, R., and Hawes, C. (1996). Brefeldin A effects in plant and fungal cells: Something new about vesicle trafficking? J. Microsc. *181*, 162–177.
21. Berleth, T., Mattsson, J., and Hardtke, C.S. (2000). Vascular continuity and auxin signals. Trends Plant Sci. *5*, 387–393.
22. Steinmann, T., Geldner, N., Grebe, M., Mangold, S., Jackson, C.L., Paris, S., Galweiler, L., Palme, K., and Jurgens, G. (1999). Coordinated polar localisation of auxin efflux carrier PIN1 by GNOM ARF GEF. Science *286*, 316–318.
23. Geldner, N., Friml, J., Stierhof, Y.-D., Jürgens, G., and Palme, K. (2001). Auxin transport inhibitors block PIN1 cycling and vesicle trafficking. Nature *413*, 425–428.
24. Satiat-Jeunemaitre, B., and Hawes, C. (1992). Redistribution of a Golgi glycoprotein in plant cells treated with Brefeldin A. J. Cell Sci. *103*, 1153–1166.
25. Ulmasov, T., Murfett, J., Hagen, G., and Guilfoyle, T.J. (1997). Aux/IAA proteins repress expression of reporter genes containing natural and highly active synthetic auxin response elements. Plant Cell *9*, 1963–1971.
26. Edlund, A., Eklof, S., Sundberg, B., Moritz, T., and Sandberg, G. (1995). A microscale technique for gas-chromatography mass-spectrometry measurements of picogram amounts of indole-3-acetic acid in plant tissues. Plant Physiol. *108*, 1043–1047.
27. Molendijk, A.J., Bischoff, F., Rajendrakumar, C.S., Friml, J., Braun, M., Gilroy, S., and Palme, K. (2001). *Arabidopsis thaliana* Rop GTPases are localized to tips of root hairs and control polar growth. EMBO J. *20*, 2779–2788.
28. Pickett, F.B., Wilson, A.K., and Estelle, M. (1990). The *aux1* mutation of *Arabidopsis* confers both auxin and ethylene resistance. Plant Physiol. *94*, 1462–1466.
29. Roman, G., Lubarsky, B., Kieber, J.J., Rothenberg, M., and Ecker, J.R. (1995). Genetic analysis of ethylene signal transduction in *Arabidopsis thaliana*: five novel mutant loci integrated into a stress response pathway. Genetics *139*, 1393–1409.
30. Willemsen, V., Wolkenfelt, H., Vrieze, G., Weisbeek, P., and Scheres, B. (1998). The *HOBBIT* gene is required for formation of the root meristem in the *Arabidopsis* embryo. Development *125*, 521–531.